Journal of NAMP 68, 1 (2024) 83-96

The Nigerian Association of Mathematical Physics

Journal homepage: https://nampjournals.org.ng

DIMENSIONLESS PRESSURE AND PRESSURE DERIVATIVE RESPONSES OF A VERTICAL WELL COMPLETED IN A RESERVOIR WITH INCLINED IMPERMEABLE EXTERNAL BOUNDARIES

[1]U.E. Emayomi and [2]E.S. Adewole

Department of Petroleum Engineering, University of Benin, Benin City, Edo State, Nigeria

ARTICLE INFO

Article history:
Received xxxxx
Revised xxxxx
Accepted xxxxx
Available online xxxxx

Keywords:
Dimensionless Pressure and Derivative Responses, Vertical Well, Inclined Sealing Boundaries.

ABSTRACT

The best well location for optimum oil production is achieved if the well either does not feel any external boundary, or the external boundary is felt much later in the life of the well. Dimensionless pressure and their derivatives are used to determine the time optimum oil production is possible for a well. For a vertical well located between two inclined impermeable boundaries, dimensionless pressures and their derivatives are computed for any angle of inclination in this paper. This is achieved using dimensionless pressure and dimensionless pressure derivative of the object vertical well, using the principle of superposition. The image distances are calculated graphically. Effects of skin and wellbore storage, are considered.

Dimensionless pressures and their gradients are affected by image distances from the object well. Images farther away from the object well present lower dimensionless pressures, and vice versa. For both faults sealing and n images, dimensionless pressure gradient and dimensionless pressure derivative are 1.151(n+1) per cycle and 0.5(n+1), respectively for a vertical well, at late flow dimensionless time for all inclination angles and image distances. A larger positive skin effect indicates additional resistance to flow, while lower values implied enhance productivity.

1. Introduction

Every reservoir has external boundaries, which may be sealing, infinite-acting, or constant-pressured. Reservoir boundaries generally affect the amount of fluid that can be produced through a well drilled into the reservoir, depending on the nature of the external boundary. Although, a reservoir may have a single or mixed external boundary combination, well location is usually decided to achieve optimum production from the well, or injection into the reservoir. The best well location is achieved if the well either does not feel any external boundary, or the external boundary is felt much later in the life of the well.

*Corresponding author: U.E. Emayomi
E-mail address: emmanuel.emayomi@eng.uniben.edu
https://doi.org/10.60787/10.60787/jnamp.v68no1.422

The type of reservoir boundary characterizes the length of time the transient can spread through the reservoir. Eventually, the transients are reached, and further propagation is stopped. Stoppage of propagation translates to cessation of further oil production. Infinite-acting reservoirs would ensure continuous propagation of the pressure transients, and, therefore continuous production of oil, since the boundaries are infinitely far away. However, no reservoir is infinitely large.

Horner [1] utilized transient pressure build up data to estimate the distance from a fault from a vertical wellbore. Davis and Hawkins [2] also utilized pressure transients pressure drawdown data to detect linear boundaries and, in addition, gave an algorithm for calculating the distance of the barrier from a wellbore. Prasad [3], investigated the pressure transient behavior of a well near two intersecting faults, and estimate numerous reservoir parameters, such as the flow capacity, reservoir pressure, the angle of inclination of the faults, and the relative distance to the fault by applying the least squares approach. A study by R. Trabelsi et al [4], attempted to describe the behavior of a well situated between a sealing fault and a constant pressure boundary. Three different slopes could be seen in their type curve results. The presence of the no-flow or sealing boundary was indicated by the second slope, the flow in an infinite reservoir by the first slope, and the presence of a constant pressure boundary by the third slope. Additionally, they noticed that when the active or object well gets closer to the sealing fault, there is a noticeable rise in the rapidity of pressure loss, leading expedited cessation of further fluid production.

Ogilvie et al [5] also reported the behavior of a well situated between a pair of sealing faults and a constant pressure boundary. References [6-13] describe dimensionless pressure and derivative behaviour for some specific angles of a reservoir with sealing external boundaries, showing the character of multiple slopes on plots of dimensionless pressures and derivatives versus log of dimensionless time. The number and magnitude of the slopes depend on the angle of inclination of the sealing faults. The transient flow regime, which is a term used to describe the behavior of wells in an infinite reservoir, characterizes the initial slope of dimensionless pressure and derivative plots.

This paper investigates the performance of a vertical well within a pair of sealing reservoir boundaries at any angle of inclination. The performance indicators are the dimensionless pressure and dimensionless pressure derivatives of the vertical well during fluid production in real time as a function of distance of object well from the inclined sealing boundaries. The effects of near wellbore problems, like wellbore skin and storage are considered. Transient flow period is assumed to prevail throughout flow period for all the cases considered.

Image Well Location Procedure for Inclined Boundaries

Figure 1 shows the object well location between a pair of sealing boundaries inclined at angle, θ. A vertical well, referred to as the object, located between the boundaries will produce number of images inversely proportional to the angle of inclination. These images act to stop pressure transients generated within the wellbore like echoes. For sealing boundaries, all the images carry positive signs. By the principle of lateral inversion, the distance of an object vertical well is the same as the image well from the boundary. All the images are located using the following procedure.

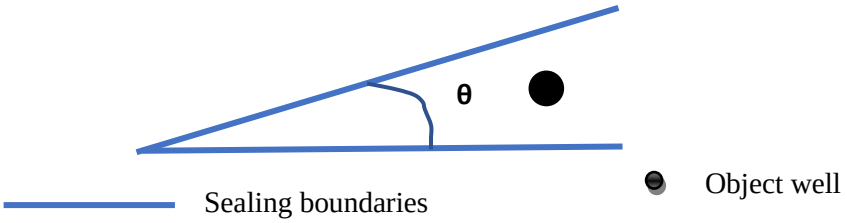

Figure 1: Well Located within a Pair of Inclined Sealing Boundaries

In counterclockwise sense,

1. Reproduce the boundaries and inclination to form a polygon of sides 360/θ.
2. Between the inclined boundaries, locate the object well at a distance d_1 from the top boundary.
3. Draw a line from the object well to hit the upper mirror (sealing boundary) at 90^0. Then the first image is at a distance of $2d_1$ away from the object well.
4. At the first image, hit the next boundary, again at 90^0.
5. Repeat Step 4 until the last image well becomes the object to the bottom boundary. The distance of the object well and the last image should be twice the distance between the object well and the bottom boundary.
6. Finally, measure the distance of each image from the object well.

If the object well distances from the boundaries are equal, a regular polygon is obtained. Otherwise, an irregular polygon is obtained. Apart from graphical procedure described above, trigonometry can also be used to calculate all the image distances.

Methodology

The number, n of images produced by a well completed within a pair of sealing boundaries inclined at an angle, θ, is given as

$$n = \frac{360}{\theta} - 1 \quad \text{……. ……1.}$$

The principle of superposition states that, the total dimensionless pressure drop in the object well is equal to dimensionless pressure drop in the object well due to flow in the object well + the sum of pressure drops in each of the image wells[14]. That is, for n image wells,

$$\Delta p_{T,0w} = \Delta p_{o,w} + \Delta p_{o,d_1} + \Delta p_{o,2} + \Delta p_{o,d_3} + \cdots \ldots\ldots + \Delta p_{o,n} \qquad 2$$

If the distances between the images and the object well are d_1, d_2, d_3, ……,d_n, then, using pressure drop expressions[11],

$$\Delta p_{T,0w} = -\frac{70.6 q_{ow} \mu B}{kh}\left[Ei\left(-\frac{946\mu\phi c_t {r_{ow}}^2}{kt}\right) - 2s + \sum_{i=1}^{n} Ei\left(-\frac{946\mu\phi c_t d_i^2}{kt}\right)\right] \qquad 3$$

In dimensionless form, this means, mathematically, that,

$$p_{DOw} = p_{DOw,Ow} + \sum_{i=1}^{n} p_{DOw,Iwi} \qquad 4$$

For a vertical well,

$$p_{Dow} = -\frac{1}{2}\left[\mathrm{Ei}\left(-\frac{1}{4t_D/c_D}\right) - 2s_{ow} + \sum_{i=1}^{n} \mathrm{Ei}\left(-\frac{d_{DIwi}^2}{4t_D}\right)\right] \qquad 5$$

Dimensionless pressure derivative is given as

$$p'_D = t_D \frac{\partial p_D}{\partial t_D/c_D} \qquad 6$$

Therefore, the dimensionless pressure derivative from Equation 1 is derived as:

$$p'_D = \frac{1}{2}\left[\exp\left(-\frac{1}{4t_D/c_D}\right) + \sum_{i=1}^{n} \exp\left(-\frac{d_{DIw1}^2}{4t_D}\right)\right] \quad 7$$

Results and Discussion

In Equation 5, Ei(-x) = $\ln(1.781x)$, when $x \leq 0.01$. But, for $x > 0.01$, Ei(-x) is evaluated according to a procedure discussed in Adewole, et al[15], or evaluated using Gauss-Laguerre quadrature procedure[16]

At large dimensionless times, the arguments of the Ei function becomes less than 0.01, Hence, at such dimensionless times, no matter how large the object and image well distances, Equation 3 can be expressed as follows:

$$p_{Dow} = -\frac{1}{2}\left[\ln\left(\frac{r_{wD}^2}{4t_D/c_D}\right) - 2s_{ow} + \sum_{i=1}^{n} \ln\left(\frac{1.781 d_{DIwi}^2}{4t_D}\right)\right] \quad 6$$

Or,

$$p_{Dow} = -1.1513\left[\left[\ln(r_{wD}^2) - \log(t_D) + \log c_D + \log({d_{D1}}^2 {d_{D2}}^2 \ldots . {d_{Dn}}^2) - n\log t_D + n\log 1.781 + 0.87 s_{ow}\right]\right] \quad 7$$

The slope of Equation (7) is the dimensionless pressure gradient derived as

$$\frac{\partial p_{ow}}{\partial \log t_D} = 1.1513(1+n) \quad 8$$

From Equation 5, also at late time flow dimensionless time, when each of the exponential term becomes zero, then

$$p'_{Dow} = 0.5(n+1) \quad 9$$

Dimensionless wellbore radius r_{wD} = 1 throughout. Assuming an equal distance, d = 0.70ft from each of the two mirrors (boundaries). Because of this equal distance, regular polygons would be produced. For 45^0 inclination, 7 images are produced according to Equation 1. Figure 2 shows the object well position, and image well locations for the 45^0 inclination case.

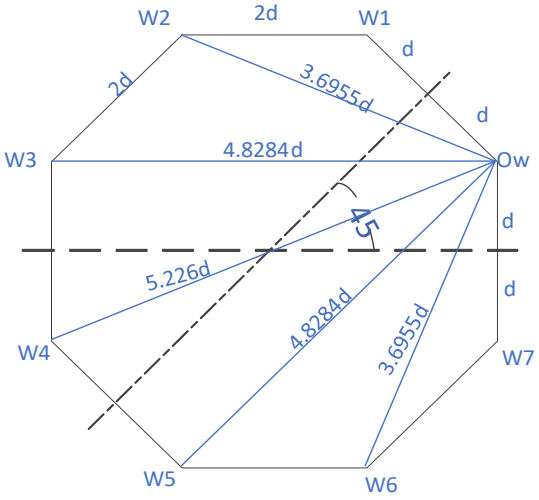

Figure 2: Object well position, and image well locations for the 45^0 inclination case[8]

From Figure 2, it is shown that from measurement and trigonometry that: d_1=2d, d_2=3.6599d, d_3=4.8284d, d_4=5.226d, d_5=4.8284d, d_6=3.6599d, d_7=2d. Results of p_D for several t_D are shown in Table 1 and Figure 3, for values of skin, s =5 and constant cD = 1, using equations 5 and 7.

Table 1: Dimensionless Pressure and Dimensionless Pressure Derivative for 45^0 inclination skin, s = 5 , cD = 1

tD	pD	p'D
0.01	2.5	6.94E-12
0.1	2.513749	0.048489
1	3.720655	1.335818
10	9.544827	3.459618
100	18.24576	3.940708
1000	27.40248	3.994014
10000	36.60743	3.999401
100000	45.81723	3.99994
1000000	55.02752	3.999994
10000000	64.23785	3.999999
1E+08	73.44819	4
1E+09	82.65853	4
1E+10	91.86887	4

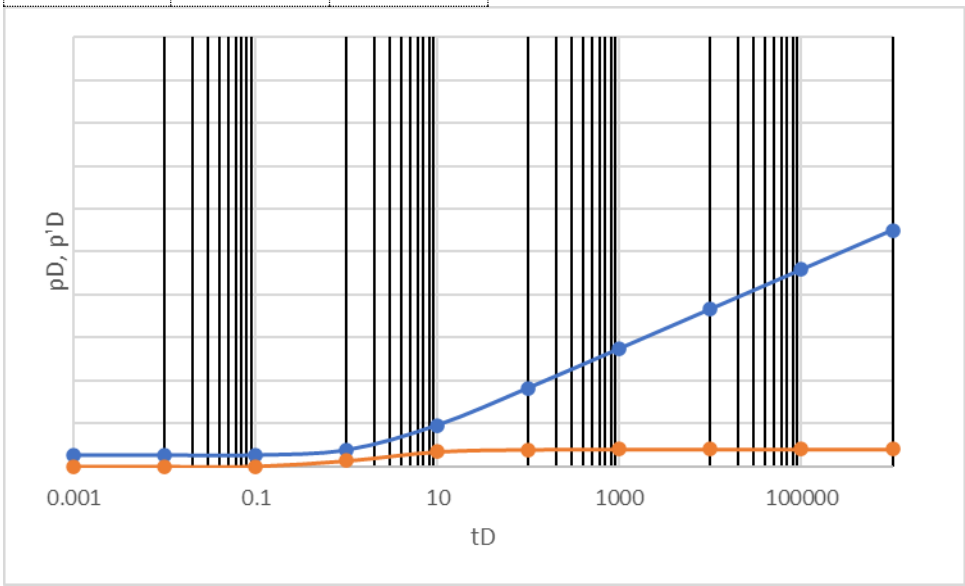

Figure 3: Dimensionless Pressure and Dimensionless Pressure Derivative for 45^0 inclination, skin, s = 5 and cD = 1

Results of p_D for several t_D are shown in Table 2 and Figure 4, for values of skin, s =0 and constant cD = 1.

Table 2: Dimensionless Pressure and Dimensionless Pressure Derivative for values of skin, s =0 and constant cD = 1.

tD	pD	p'D
0.001	5.3E-112	1.3E-109
0.01	2.67E-13	6.94E-12
0.1	0.013749	0.048489
1	1.220655	1.335818

10	7.044827	3.459618
100	15.74576	3.940708
1000	24.90248	3.994014
10000	34.10743	3.999401
100000	43.31723	3.99994
1000000	52.52752	3.999994
10000000	61.73785	3.999999
1E+08	70.94819	4
1E+09	80.15853	4
1E+10	89.36887	4

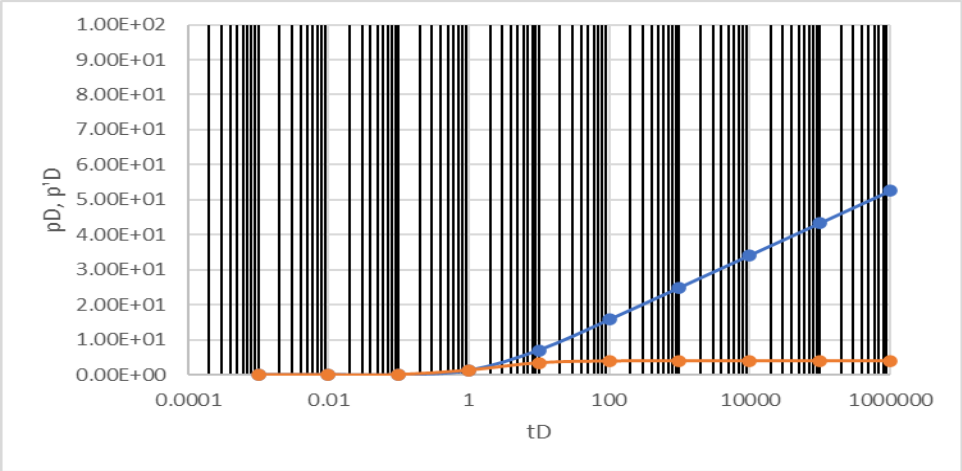

Figure 4: Dimensionless Pressure and Dimensionless Pressure Derivative for 45^0 inclination, skin, s = 0 and cD = 1

From the results in Table 1 and Figure 3, at late dimensionless time, dimensionless pressure gradient is 91.86887 - 82.65853 = 9.2103 per cycle. From Equation 8, n = 7, confirming the number of images, and therefore, inclination angle of 45^0 from Equation 1. Furthermore, dimensionless pressure derivative of 4 confirms n =7 from Equation 9.

Figure 5 shows the case of boundaries inclination at 60^0. Five images are produced. Results of dimensionless pressure and dimensionless pressure derivative are shown in Table 3 and 4 and Figure 6 and 7 for different case of wellbore storage and skin..

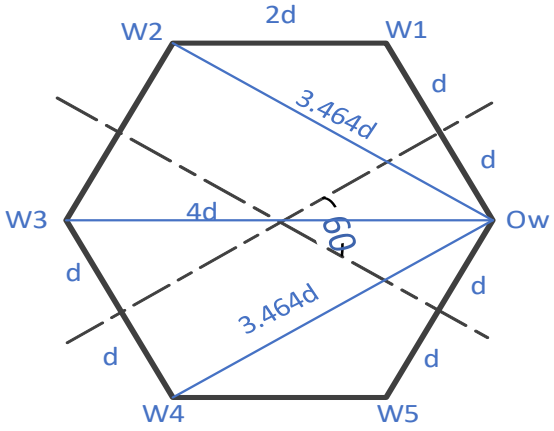

Figure 5: Object well position, and image well locations for the 60^0 inclination case

Table 3: Dimensionless Pressure and Dimensionless Pressure Derivative for 60^0 inclination s =5, cD = 1

tD	pD	p'D
0.001	2.5	1.3E-109
0.01	2.5	6.94E-12
0.1	2.513749	0.04849
1	3.725599	1.303742
10	8.660341	2.714646
100	15.30313	2.969625
1000	22.18346	2.996943
10000	29.08846	2.999694
100000	35.99594	2.999969
1000000	42.90367	2.999997
10000000	49.81142	3
1E+08	56.71918	3
1E+09	63.62693	3
1E+10	70.53469	3

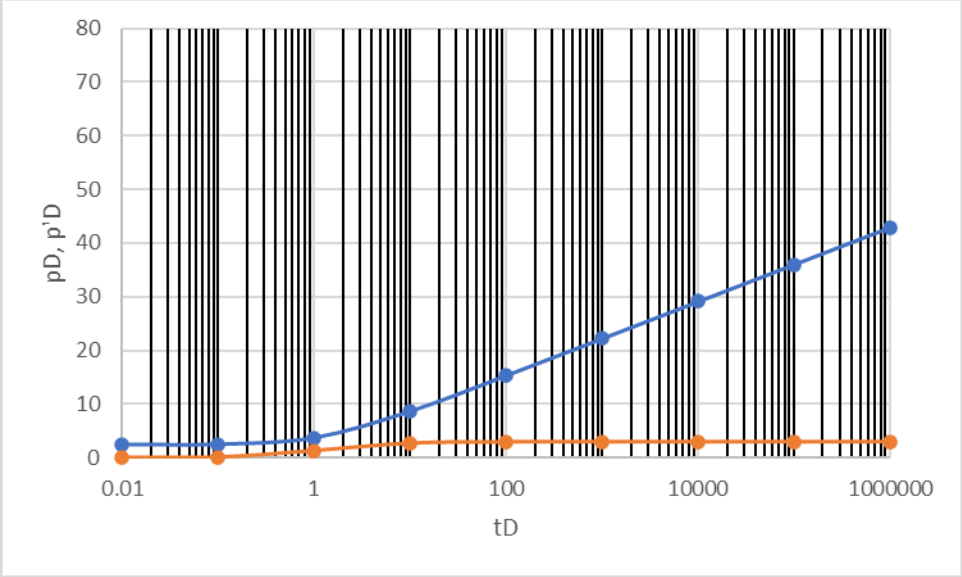

Table 6: Dimensionless Pressure and Dimensionless Pressure Derivative for 60^0 inclination s =5, cD = 1

Table 4: Dimensionless Pressure and Dimensionless Pressure Derivative for 60^0 inclination s = -0.5, cD = 1

tD	pD	p'D
0.001	-0.25	1.3E-109
0.01	-0.25	6.94E-12
0.1	-0.23625	0.04849
1	0.975599	1.303742
10	5.910341	2.714646
100	12.55313	2.969625
1000	19.43346	2.996943
10000	26.33846	2.999694
100000	33.24594	2.999969

1000000	40.15367	2.999997
10000000	47.06142	3
1E+08	53.96918	3
1E+09	60.87693	3
1E+10	67.78469	3

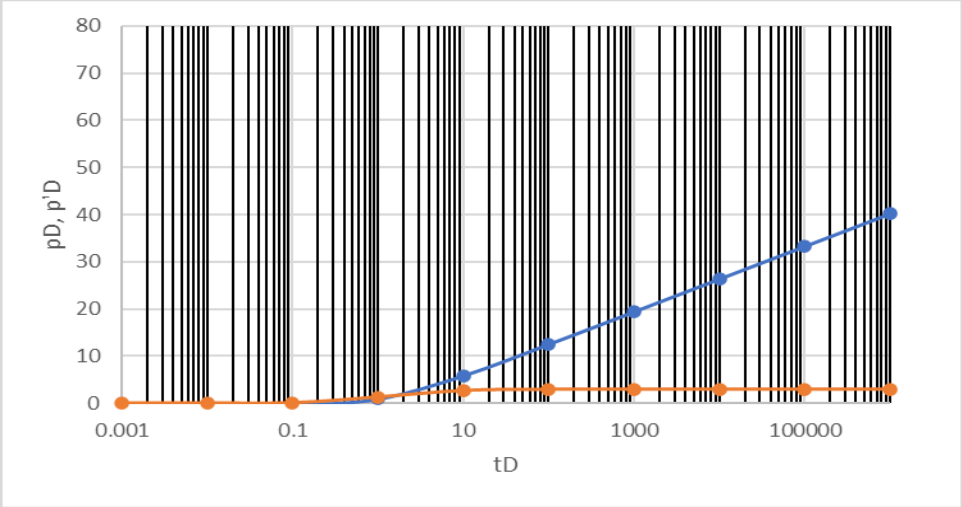

Figure 7: Dimensionless Pressure and Dimensionless Pressure Derivative for 60^0 inclination s = -0.5, cD = 1

Figure 8 shows the case of boundaries inclination at 90^0. Three images are produced. Results of dimensionless pressure and dimensionless pressure derivative are shown in Table 5 and 6 and Figure 8 and 9 for different case of wellbore storage and skin..

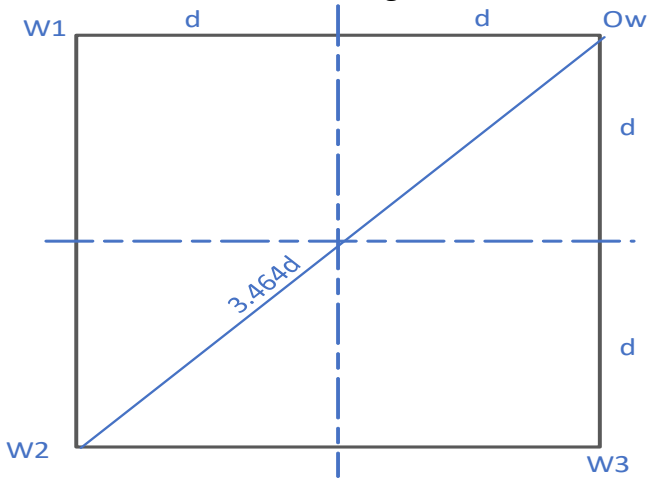

Figure 8: Object well position, and image well locations for the 90^0 inclination case[12-13]

Table 5: Dimensionless Pressure and Dimensionless Pressure Derivative for 90^0 inclination s = 10, cD = 1

tD	pD	p'D
0.001	5	1.3E-109
0.01	5	6.94E-12
0.1	5.013749	0.048489
1	6.146992	1.11767
10	9.798054	1.871738

100	14.28522	1.986596
1000	18.8783	1.998654
10000	23.48226	1.999865
100000	28.08731	1.999987
1000000	32.69247	1.999999
10000000	37.29764	2
1E+08	41.90281	2
1E+09	46.50798	2
1E+10	51.11315	2

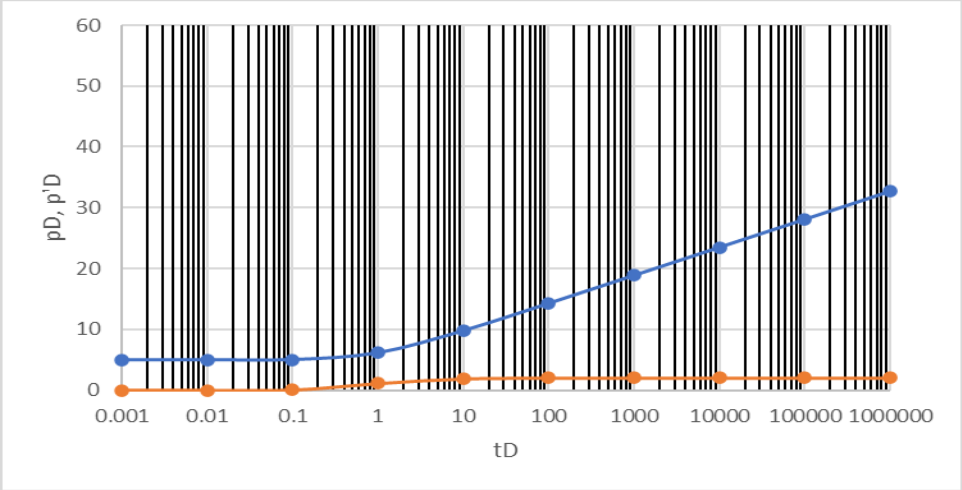

Table 9: Dimensionless Pressure and Dimensionless Pressure Derivative for 90^0 inclination s = 10, cD = 1

Table 6: Dimensionless Pressure and Dimensionless Pressure Derivative for 90^0 inclination s = 0, cD = 1

tD	pD	p'D
0.001	5.3E-112	1.3E-109
0.01	2.67E-13	6.94E-12
0.1	0.013749	0.048489
1	1.146992	1.11767
10	4.798054	1.871738
100	9.285223	1.986596
1000	13.8783	1.998654
10000	18.48226	1.999865
100000	23.08731	1.999987
1000000	27.69247	1.999999
10000000	32.29764	2
1E+08	36.90281	2
1E+09	41.50798	2
1E+10	46.11315	2

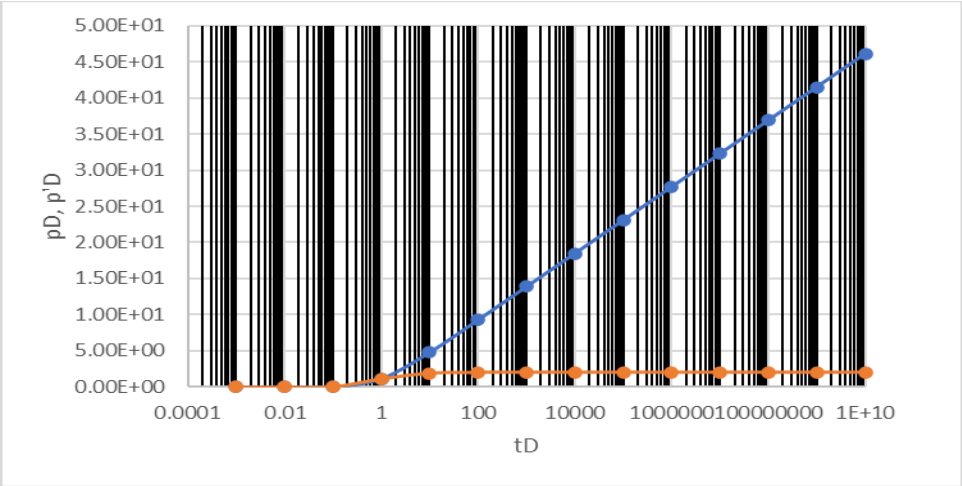

Figure 10: Dimensionless Pressure and Dimensionless Pressure Derivative for 90^0 inclination s = 0, cD = 1

Figure 11 shows the case of boundaries inclination at 120^0. Two images are produced. Results of dimensionless pressure and dimensionless pressure derivative are shown in Table 7 and 8 and Figure 12 and 13 for different case of wellbore storage and skin.

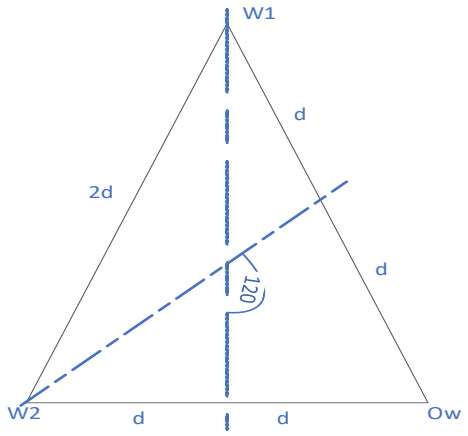

Figure 11: Case of boundaries inclination at 120^0

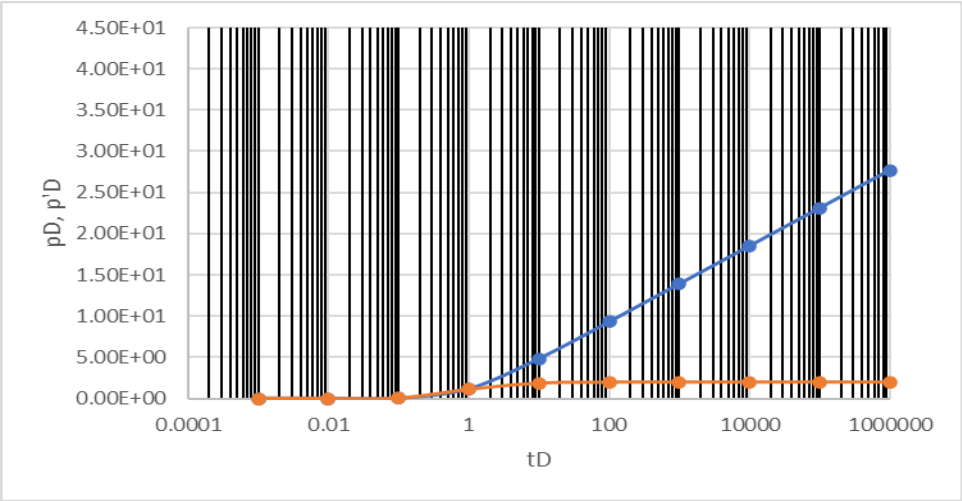

Figure 12: Dimensionless Pressure and Dimensionless Pressure Derivative for 120^0 inclination s = -0.5, cD = 1

Table 7: Dimensionless Pressure and Dimensionless Pressure Derivative for 120^0 inclination s = -0.5, cD = 1

tD	pD	p'D
0.001	-0.25	1.3E-109
0.01	-0.25	6.94E-12
0.1	-0.23625	0.048489
1	0.84423	1.002027
10	3.80538	1.439836
100	7.204572	1.493864
1000	10.65292	1.499385
10000	14.10625	1.499939
100000	17.56007	1.499994
1000000	21.01394	1.499999
10000000	24.46782	1.5
1E+08	27.92169	1.5
1E+09	31.37557	1.5
1E+10	34.82945	1.5

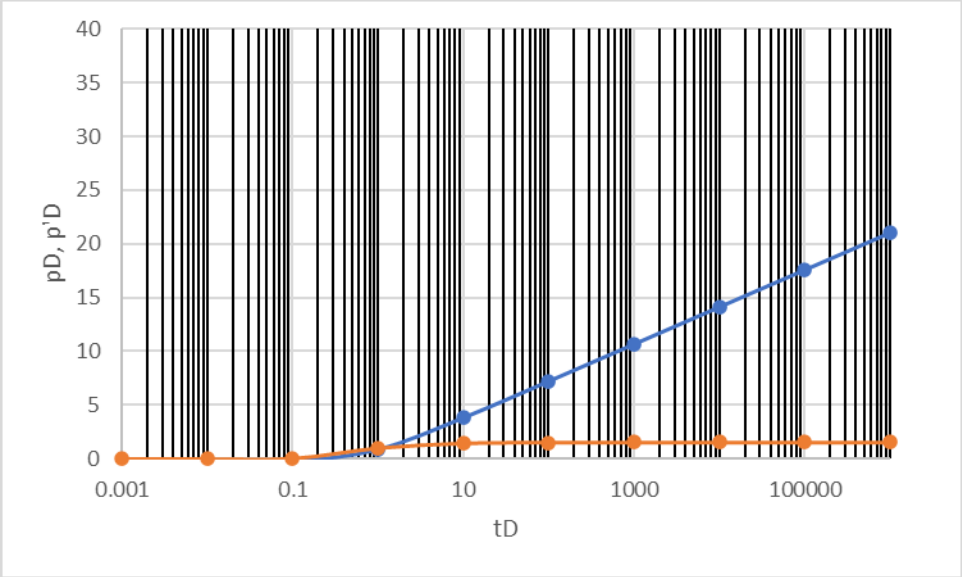

Figure 13: Dimensionless Pressure and Dimensionless Pressure Derivative for 120^0 inclination s = 3, cD = 1

Table 8: Dimensionless Pressure and Dimensionless Pressure Derivative for 120^0 inclination s = 3, cD = 1

tD	pD	p'D
0.001	1.5	1.3E-109
0.01	1.5	6.94E-12
0.1	1.513749	0.048489
1	2.59423	1.002027
10	5.55538	1.439836
100	8.954572	1.493864

1000	12.40292	1.499385
10000	15.85625	1.499939
100000	19.31007	1.499994
1000000	22.76394	1.499999
10000000	26.21782	1.5
1E+08	29.67169	1.5
1E+09	33.12557	1.5
1E+10	36.57945	1.5

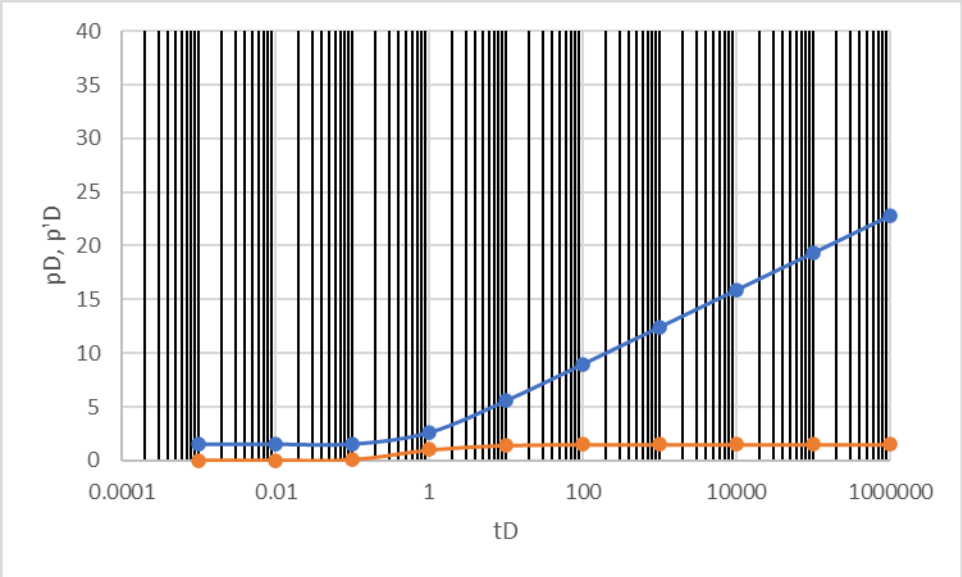

Figure 14: Dimensionless Pressure and Dimensionless Pressure Derivative for 120^0 inclination s = 3, cD = 1

From the results tabulated, there is a progressive increase in dimensionless pressure and that of the derivative as the dimensionless time increases. More so, the higher the fault angle, the lower the distance required to produce the well optimally at a given time of production.
From Equations (8) and (9), the dimensionless pressure gradient and dimensionless pressure derive do not depend on well distances at long flow dimensionless time. Since the fault starts to exert its influence at that point, all of the slopes were obtained in the extremely late dimensionless time.
A larger positive skin effect indicates additional resistance to flow(higher p_D) , while negative skin imply enhanced productivity(lower p_D). Larger wellbore storage delays attainment of both early and late flow periods[8-10] .

Conclusion

In this work, successful mathematical models were constructed for determining the angle of inclination of a well finished within two inclined sealing faults, as well as for calculating dimensionless pressure and dimensionless pressure derivative.

1. At early flow dimensionless time, dimensionless pressure and their derivative responses vary according to the different angles, object and image well location and distances from the object well, respectively, well type and angle of inclination of reservoir sealing external boundaries.
2. At long flow dimensionless time, dimensionless pressure and their derivative responses are dependent only on angle of inclination of the external sealing boundaries and well type.

3. At all flow dimensionless time, dimensionless pressures and their derivatives are independent on the vertical well design.
4. For n images, dimensionless pressure gradient and dimensionless pressure derivative are 1.151(n+1) per cycle and 0.5(n+1), respectively for a vertical well, at late flow dimensionless time for all inclination angles and image distances.
5. A larger positive skin effect indicates additional resistance to flow, while negative skin imply enhanced productivity.
6. Larger wellbore storage delays attainment of both early and late flow periods.

Nomenclature

$p_D = \frac{kh\Delta p}{141.2q\mu B}$

$t_D = \frac{0.000264kt}{\phi\mu c_t r^2}$

$r_D = \frac{r}{r_w}$

$r_{wD} = \frac{r_w}{r_w} = 1$

$\Delta p = p_i - p_w$

p_D Dimensionless pressure

$p_{D'}$ Dimensionless pressure derivative

p_i Initial reservoir pressure, psi

p_w Wellbore pressure, psi

tD Dimensionless time

q_o Stabilized oil flow rate before shut-in, STB/day

r_w Wellbore radius (ft)

k Reservoir permeability (mD)

ϕ Reservoir porosity

μ Fluid viscosity (cp)

c_t Total compressibility (1/psi)

q Production rate (stb/day)

B Formation volume Factor (bbl/stb)

h Average reservoir thickness (ft)

$\Delta p_{T,o}$ Total pressure drop in the object well

d Distance of image well from object well.

n Number of images

m Gradient (per cycle)

Θ Angle of inclination (degree)

Ow Object well

wn nth image well

s Skin factor

References

[1] Horner, D. R.: Pressure Build-Up in Wells. published in the Transactions of the American Institute of Mining, Metallurgical, and Petroleum Engineers (AIME), 1951.

[2] Davis, E.G. and Hawkins, M.F.: "Linear Fluid-Barrier Detection by Well Pressure Measurements", Journal of Petroleum Technology, 15, 1963, 1077-1081.

[3] Prasad: "Pressure Trasient Behavior of a well Near Two Intersecting Limits", Journal of Petroleum Technology, 1975.

[4] R. Trabelsi et al: "Behavior of a well located between a Sealing Fault and a Constant Pressure Boundary", Journal of Petroleum Technology, 2017.

[5] Ogilvie, S.R. , Dee, S. J. Wilson, R. W., and Wayne R.: "Integrated Fault Seal Analysis", July 17, 2020**,** The Geological Society of London.

[6] Adewole, E.S.: "Applications of Superposition Principle in Oil and Gas Well Management", Lecture presented in the Lecture Series of Society of Petroleum Engineers, Section 116, Benin City, Virtual, Nigeria, May 14, 2020.

[7] Adewole, E.S.:"Signatures of a Horizontal Well Completed Near a Sealing Boundary", Lecture presented in the Lecture Series of Society of Petroleum Engineers, Lagos Section 61, Lecture Series, Virtual, March 2021.

[8] Eziuzor, D.T. and Adewole, E.S. :"Type Curves of a Vertical Well Completed within a Pair of Inclined Sealing Faults", Paper presented at the SPE Nigeria Annual International Conference and Exhibition, Lagos, Nigeria, August 01, 2022.

[9] Yakubu, B.O. and Adewole, E.S.: "Dimensionless Pressure and Derivative Responses of a Vertical Well in a Reservoir with Impermeable Boundaries Inclined at Right Angle" *Journal of Engineering for Development*, vol. 16, March 2024, pp. 95-109, https://jedev.com.ng/volume-16.

[10] Olokor, W.F. and Adewole, E.S.: "Pressure and Derivative Responses of a Horizontal Well in a Reservoir with Impermeable Boundaries Inclined at Right Angle," *Journal of Engineering for Development*, vol. 16, March 2024, pp. 110-129, https://jedev.com.ng/volume-16.

[11] Britton, P.R. and Grader, A.S.: "The Effects of Size, Shape, and Orientation of an Impermeable Region on Transient Pressure Testing", *SPE Formation Evaluation*, 3, 1988, p.595-606.

[12] Johnson J. and Adewole, E. "Flow Behavior of Horizontal Well Completed within Two Sealing Faults Inclined at Right Angle", August 2, 2021.

[13] Lee, J., Rollins, J. B., and Spivey, J. P.: *Well Test Analysis*; Society of Petroleum Engineer,1989.

[14] Earlougher, R.C.Jr: *Advances in Well Test Analysis*, Society of Petroleum Engineers Monograph, 1977.

[15] Adewole, E.S. and Bello, K.O.: "Application of Gauss-Laguerre Quadrature in Computing Exponential Integral Functions, E" SPE 98829, paper paper presented at the Society of Petroleum Engineers Annual International Conference and Exhibition, Abuja, August 1-3, 2006.

[16] Carnahan, B., Luther, H.A., and Wilkes, J.O.: *Applied Numerical Methods*, John Wiley and Sons, 1969.